ROME 2008
LEVERAGING TECHNOLOGY

H034

Parsimonious Finite-volume Frequency-domain Method for 2D P-SV-wave Modelling

R. Brossier* (Univ. Nice Sophia-Antipolis, Geosciences Azur), J. Virieux (Univ. Joseph Fourier, LGIT) & S. Operto (CNRS, Geosciences Azur)

SUMMARY

A new numerical technique for solving the 2D elastodynamic equations in the frequency domain based on a finite-volume P0 approach is proposed for application to full waveform inversion. The associated discretisation is through triangles and the free surface is described along the edges of the triangles which may have different slopes. By applying a parsimonious strategy, only velocity fields are left as unknowns in triangles, minimizing the core memory requirement of the simulation. Efficient PML absorbing conditions have been designed for damping waves around the grid. The method is validated against analytical solutions of several canonical problems and with numerical solutions computed with a well-established finite-difference time-domain method in heterogeneous media. In presence of a free surface, the finite-volume method requires ten triangles per wavelength for a flat topography and fifteen triangles per wavelength for more complex shapes, well below criteria required by the staircase approximation of finite-difference methods. Comparison between the frequency-domain finite-volume and the second-order rotated finite-difference methods also shows that the former is faster and less-memory demanding for a given accuracy level, an encouraging point for application of full waveform inversion in realistic configurations.

Introduction

Since the success of the full waveform inversion in the frequency domain (Pratt and Worthington, 1990), applications to real data using the acoustic approximation have been performed for imaging complex structures (Operto *et al.* , 2006) while reconstruction of elastic parameters is still a quite challenging problem (Gelis *et al.* , 2007). For elastic full-waveform inversion in realistic configurations, an efficient method must be developed in the frequency domain for modelling elastic waves in heterogeneous media with a free surface of arbitrary shape.
Seismic wave propagation has been investigated with various numerical methods such as finite-difference (FD), finite-element (FE) or boundary integral equations (BIE). The FD method is quite popular and have been intensively used for forward modelling as well as for seismic imaging but requires a high number of grid points per wavelength for minimal numerical dispersion especially nearby the free surface described by staircase approximation (Bohlen and Saenger, 2006). Finite Volume approaches (FV) have been recently developed by BenJemaa *et al.* (2007); Käser and Dumbser (2006) with promising perspectives.
We have developed a parsimonious FV frequency-domain method for the 2D velocity-stress P-SV wave equation which allows a dense sampling of the mesh nearby the free surface. Absorbing boundary conditions are designed through the Perfectly-Matched Layers (PML) approach (Berenger, 1994). The method is validated both against analytical and numerical solutions computed with a FD time-domain method. The numerical cost of the FV method is finally compared with that of the FD frequency-domain method before concluding on its potentialities for full-waveform inversion.

Finite Volume Formulation

We consider first-order hyperbolic elastodynamic system for 2D P-SV waves in isotropic medium in the frequency domain where both velocities (V_x,V_z) and stress (σ_{xx},σ_{zz},σ_{xz}) are unknown quantities as described by the following differential system,

$$\begin{aligned}
-\imath\omega V_x &= \frac{1}{\rho(\mathbf{x})}\Big\{\frac{\partial \sigma_{xx}}{\partial x}+\frac{\partial \sigma_{xz}}{\partial z}\Big\}+F_x \\
-\imath\omega V_z &= \frac{1}{\rho(\mathbf{x})}\Big\{\frac{\partial \sigma_{xz}}{\partial x}+\frac{\partial \sigma_{zz}}{\partial z}\Big\}+F_z \\
-\imath\omega \sigma_{xx} &= \big(\lambda(\mathbf{x})+2\mu(\mathbf{x})\big)\frac{\partial V_x}{\partial x}+\lambda(\mathbf{x})\frac{\partial V_z}{\partial z}-\imath\omega\sigma_{xx_0} \\
-\imath\omega \sigma_{zz} &= \lambda(\mathbf{x})\frac{\partial V_x}{\partial x}+\big(\lambda(\mathbf{x})+2\mu(\mathbf{x})\big)\frac{\partial V_z}{\partial z}-\imath\omega\sigma_{zz_0} \\
-\imath\omega \sigma_{xz} &= \mu(\mathbf{x})\Big\{\frac{\partial V_x}{\partial z}+\frac{\partial V_z}{\partial x}\Big\}-\imath\omega\sigma_{xz_0},
\end{aligned} \tag{1}$$

where Lamé coefficients are denoted by λ, μ, the density by ρ and the angular frequency by ω. Physical model is represented by a distribution of triangle cells in a conformal mesh (three edges and neighbours are imposed for each cell). Finite Volume method is applied to the weak formulation of system 1 as usually done for FV formulation with introduction of centered numerical fluxes (Remaki, 1999; BenJemaa *et al.* , 2007). FV P_0 assumption imposed that solutions are piecewise constant in each cell. Perfectly Matched Layer (Berenger, 1994) are introduced to avoid parasite reflections on model boundaries. To minimise the number of unknowns, stress components are eliminated from the discrete equations following the parsimonious strategy first proposed by Luo and Schuster (1990). Finally, we end up with two algebraic equations (system 2) for the two unknown velocity components where i denote the current cell, A_i the area of the i cell, $j \in \partial K_i$ and $k \in \partial K_j$ label the three neighbouring cells with a common edge with the i and the j cells respectively. The length of the edge between two cells i and j is denoted by l_{ij}. n_{ij_r} denotes the normal vector component r oriented for each edge of cell i towards cell j. Terms s_{r_l} are related to PML functions.
Equations 2 can be recast in matrix form as $\mathcal{A}V = \mathcal{B}$ where the sparse impedance matrix $\mathcal{A}$

contains 14 non-zero coefficients per row in the general case (i.e., without any regular structure) due to expected irregular numbering of cells inside the mesh.(18 for FD stencil used by Gelis *et al.* (2007)). Free-surface and fluid-solid boundary conditions are explicitely expressed in this scheme by a local modification of numerical fluxes.

$$
\begin{aligned}
\omega^2 V_{x_i} &= \iota\omega F_{x_i} + \frac{\iota\omega}{A_i\rho_i}\sum_{j\in\partial K_i}\frac{l_{ij}}{2}\Big\{n_{ij_x}s_{x_j}\Big[\frac{\iota(\lambda_j+\mu_j)}{\omega A_j}\sum_{k\in\partial K_j}\frac{l_{jk}}{2}(n_{jk_x}s'_{x_k}V_{x_k}+n_{jk_z}s'_{z_k}V_{z_k})+T^0_{1_j}\Big]\\
&+ n_{ij_x}s_{x_j}\Big[\frac{\iota\mu_j}{\omega A_j}\sum_{k\in\partial K_j}\frac{l_{jk}}{2}(n_{jk_x}s'_{x_k}V_{x_k}-n_{jk_z}s'_{z_k}V_{z_k})+T^0_{2_j}\Big]\\
&+ n_{ij_z}s_{z_j}\Big[\frac{\iota\mu_j}{\omega A_j}\sum_{k\in\partial K_j}\frac{l_{jk}}{2}(n_{jk_x}s'_{x_k}V_{z_k}+n_{jk_z}s'_{z_k}V_{x_k})+T^0_{3_j}\Big]\Big\}\\
\omega^2 V_{z_i} &= \iota\omega F_{z_i} + \frac{\iota\omega}{A_i\rho_i}\sum_{j\in\partial K_i}\frac{l_{ij}}{2}\Big\{n_{ij_z}s_{z_j}\Big[\frac{\iota(\lambda_j+\mu_j)}{\omega A_j}\sum_{k\in\partial K_j}\frac{l_{jk}}{2}(n_{jk_x}s'_{x_k}V_{x_k}+n_{jk_z}s'_{z_k}V_{z_k})+T^0_{1_j}\Big]\\
&- n_{ij_z}s_{z_j}\Big[\frac{\iota\mu_j}{\omega A_j}\sum_{k\in\partial K_j}\frac{l_{jk}}{2}(n_{jk_x}s'_{x_k}V_{x_k}-n_{jk_z}s'_{z_k}V_{z_k})+T^0_{2_j}\Big]\\
&+ n_{ij_x}s_{x_j}\Big[\frac{\iota\mu_j}{\omega A_j}\sum_{k\in\partial K_j}\frac{l_{jk}}{2}(n_{jk_x}s'_{x_k}V_{z_k}+n_{jk_z}s'_{z_k}V_{x_k})+T^0_{3_j}\Big]\Big\}. \qquad (2)
\end{aligned}
$$

PML absorbing boundary conditions

Numerical tests showed that PML efficiency strongly depends on the mesh structure in the PMLs. The PML condition requires that the PML-PML interfaces are oriented along the Cartesian directions (Berenger, 1994). This condition is not verified if triangles of arbitrary orientations are used in the PML layers. In that case, we observed a poor absorption (Figure 1 (b)). Therefore, a constrained mesh in PML zones with multi-layer structure parallel to Cartesian directions (see the figure 1 (a) for the discretisation of the lower left quarter of the medium) makes catch conditions for can efficient absorption of elastic waves (Figure 1 (c)).

Numerical results

Several benchmarks were performed for assessing the accuracy of this new method with different meshes structures. The method has been validated against analytical solutions computed in homogeneous media with explosive source, for the Garvin problem and for models composed of two elastic half spaces delineated by a horizontal interface. Comparisons have also been performed with FD time-domain reference solutions computed in for more complex media: a Corner-Edge model to deal with reflection and diffraction of volume and surface waves, a hill

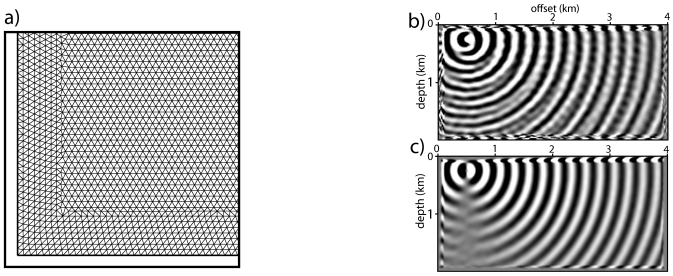

Figure 1: (a): PML construction with multi-layer structure parallel to Cartesian directions for the lower left quarter of the medium. Right side: Frequency map solutions where the real part of horizontal velocity for different PML configuration is displayed. No mesh constrains are applied on (b) whereas mesh constraints ares applied on (c).

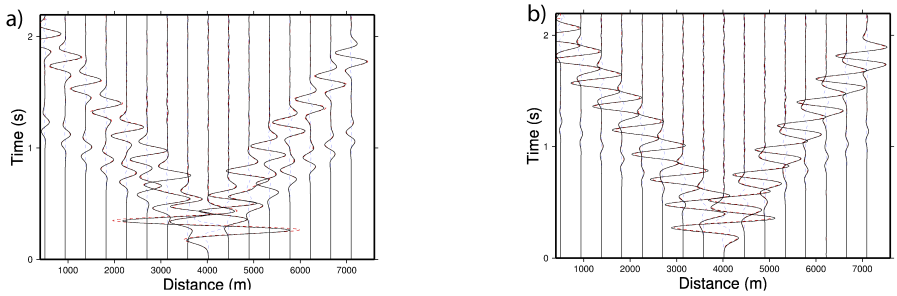

Figure 2: Seismograms computed in the hill model using equilateral and unstructured meshes. Horizontal (a) and vertical (b) components of particle velocity at receivers are illustrated. Reference solution computed with FV in regular equilateral mesh is plotted with discontinuous red lines and solution in unstructured mesh with continuous black lines. Note the time shift of the solution computed in unstructured mesh increasing with propagation time.

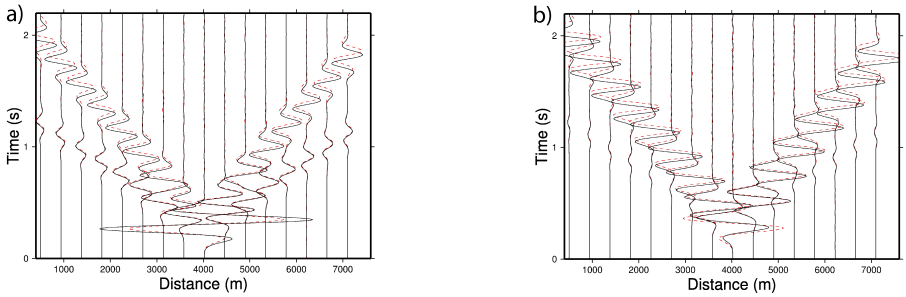

Figure 3: Seismograms computed in the hill shaped model for the horizontal (a) and vertical (b) components of velocity. Reference solution computed with the FD time-domain method is represented by discontinuous red lines, the FV solution by continuous black lines and the difference between the two solutions with discontinuous blue lines.

shaped topography above an homogeneous model and a subset of the Marmousi II model to deal with realistic heterogeneous medium. All comparisons have been performed in the time domain where reference solutions are naturally computed.

These different tests have shown a kinematic delay for unstructured meshes, related to the P_0 interpolation as illustrated in figure 2 for a simulation in the hill shaped model. Such inaccuracies have not been observed for equilateral meshes for which accurate results have been obtained for a discretisation of 10 cells and 15 cells per minimum shear wavelength when flat topography and complex shape topography are considered respectively. This discretisation is coarser than the discretization required by classical 2^{nd}-order rotated FD stencil for the same level of accuracy and the two topography configurations, that is, 25 and 60 points per wavelength respectively. Figure 3 shows comparison between FV (15 equilateral cells per S wavelength) et FD (60 points per S wavelength) seismograms for the hill shaped model where both volume and surface waves are well modeled.

A comparison of the numerical cost of the FV and second-order rotated FD methods is given in table 1. The simulation was performed in a target of the Marmousi II model representing an 6000 m x 2500 m heterogeneous model with a flat free surface. 10 cells and 28 points per shear wavelength were used for FV and FD respectively to minimise numerical dispersion. Both codes use the MUMPS direct solver to solve the linear system through LU factorization. FV is clearly less expensive for all resolution times thanks to the coarser discretization of the medium except to build-up tables relative to mesh which is implicitly done in FD.

Numerical method	regular FV	unstructured FV	FD
Number of unknowns to solve	1 421 364	549 638	4 850 020
Time to prepare data for matrix building	54.4 s	40.1 s	1.0 s
Time for matrix building	1.6 s	0.80 s	10.9 s
Time for factorisation	272.3 s	79.5 s	999.4 s
Memory use for factorisation	3448 Mb	1333 Mb	12061 Mb
Time for resolution of 1 shot	3.8 s	1.7 s	13.5 s

Table 1: Numerical cost for FV and FD in frequency domain for realistic model at 13 Hz.

Conclusion

A FV method has been formulated in the space-frequency domain for 2D P-SV wave propagation. Comparison of the FV solutions with analytic and numerical reference solutions in canonical and realistic configurations have shown that structured equilateral mesh gives accurate results for a discretisation of 10 cells per shear wavelength even if flat free surface is considered. Complex topography should require finer description of 15 cells, coarser than classical FD due to triangular meshing. CPU/memory requirements are naturally less expensive than FD in spite of complex table manipulations due to the mesh description of medium. Finally, FV method in regular meshes appears to be very efficient when compared with FD methods especially when realistic topography is considered. Considering unstructured meshes allows a significant decrease of numerical resources in spite of weaker accuracy of the wavefield estimation. Future work will focus on implementation of such method in full waveform inversion. Moreover, moving to higher order for the interpolation P_1 in the discontinuous Galerkin approach should be investigated to achieve acceptable accuracy when using unstructured meshes.

Acknowledgements

This research was funded by the SEISCOPE consortium ($http://seiscope.unice.fr$) sponsored by BP, CGG-VERITAS, EXXON-MOBIL, SHELL and TOTAL. Access to the high performance computing facilities of MESOCENTRE SIGAMM computer center provided the required computer resources.

References

BenJemaa, M., Glinsky-Olivier, N., Cruz-Atienza, V. M., Virieux, J., and Piperno, S. [2007] Dynamic non-planar crack rupture by a finite volume method. *Geophysical Journal International* 171, 271–285.

Berenger, J-P. [1994] A perfectly matched layer for absorption of electromagnetic waves. *Journal of Computational Physics* 114, 185–200.

Bohlen, T., and Saenger, E. H. [2006] Accuracy of heterogeneous staggered-grid finite-difference modeling of rayleigh waves. *Geophysics* 71, 109–115.

Gelis, C., Virieux, J., and Grandjean, G. [2007] 2D elastic waveform inversion using born and rytov approximations in the frequency domain. *Geophys. J. Int.* 168, 605–633.

Käser, M., and Dumbser, M. [2006] An Arbitrary High Order Discontinuous Galerkin Method for Elastic Waves on Unstructured Meshes I: The Two-Dimensional Isotropic Case with External Source Terms. *Geophysical Journal International* 166, 855–877.

Luo, Y., and Schuster, G. T. [1990] Parsimonious staggered grid finite-differencing of the wave equation. *Geophysical Research Letters* 17(2), 155–158.

Operto, S., Virieux, J., Dessa, J. X., and Pascal, G. [2006] Crustal imaging from multifold ocean bottom seismometers data by frequency-domain full-waveform tomography: application to the eastern nankai trough. *Journal of Geophysical Research* 111(B09306), doi:10.1029/2005JB003835.

Pratt, R. G., and Worthington, M. H. [1990] Inverse theory applied to multi-source cross-hole tomography. Part 1: acoustic wave-equation method. *Geophysical Prospecting* 38, 287–310.

Remaki, M. [1999] A new finite volume scheme for solving maxwell's system. *COMPEL* 19(3), 913–931.